

SOLVING CUBIC MATRIX EQUATIONS ARISING IN CONSERVATIVE DYNAMICS

MICHELE BENZI AND MILO VIVIANI

Dedicated to Alfio Quarteroni on his 70th Birthday

ABSTRACT. In this paper we consider the spatial semi-discretization of conservative PDEs. Such finite dimensional approximations of infinite dimensional dynamical systems can be described as flows in suitable matrix spaces, which in turn leads to the need to solve polynomial matrix equations, a classical and important topic both in theoretical and in applied mathematics. Solving numerically these equations is challenging due to the presence of several conservation laws which our finite models incorporate and which must be retained while integrating the equations of motion. In the last thirty years, the theory of geometric integration has provided a variety of techniques to tackle this problem. These numerical methods require to solve both direct and inverse problems in matrix spaces. We present two algorithms to solve a cubic matrix equation arising in the geometric integration of isospectral flows. This type of ODEs includes finite models of ideal hydrodynamics, plasma dynamics, and spin particles, which we use as test problems for our algorithms.

Keywords: Cubic matrix equations, Lie–Poisson integrator, Euler equations, Plasma vortices, Spin systems

1. INTRODUCTION

The numerical solution of polynomial matrix equations is a well studied and active field of research [1, 2, 7]. Its relevance clearly goes beyond pure mathematics and the development of efficient algorithms is crucial in several areas of computational science. Linear matrix equations have been studied since the 19th Century, beginning with Sylvester [8]. Linear matrix equations have a variety of different formulations, and according to the specific structure, different techniques can be used to solve them [2, 7]. One degree higher, we find quadratic matrix equations. For such problems the theory is more intricate and various numerical issues may appear [1]. Among the quadratic matrix equations, one of the most studied is the continuous-time algebraic Riccati equation (CARE) [1], which will appear in Section 3.

In this paper, we study the numerical solution of the cubic matrix equation

$$(I - h\mathcal{L}X)X(I + h\mathcal{L}X) = Y, \quad (1)$$

where X is unknown and Y is given in $\mathbb{M}(N, \mathbb{R})$ or $\mathbb{M}(N, \mathbb{C})$ (the spaces of $N \times N$ real or complex matrices), and \mathcal{L} is a linear operator acting on matrices. Equation (1) appears in the geometric integration of matrix flows of the form:

$$\begin{aligned} \dot{Y} &= [\mathcal{L}Y, Y], \\ Y(0) &= Y_0, \end{aligned} \quad (2)$$

where $Y = Y(t)$ is a curve in some subspace of the space $\mathbb{M}(N, \mathbb{R})$ or $\mathbb{M}(N, \mathbb{C})$ and the square brackets denote the commutator of two matrices: $[A, B] = AB - BA$. The flow of (1) is isospectral, which means that the eigenvalues of $Y(t)$ do not depend on t . Furthermore, when \mathcal{L} is self-adjoint, (1) is Hamiltonian (another term is ‘‘Lie–Poisson’’), with Hamiltonian function given by

$$H(Y) = \frac{1}{2} \text{Tr}(Y^* \mathcal{L} Y), \quad (3)$$

where $*$ denotes the transpose conjugate. A discrete approximation of the solution of (1) is determined, for $h > 0$ sufficiently small, by the implicit-explicit iteration defined in [9] as:

$$\begin{aligned} (I - h\mathcal{L}X_n)X_n(I + h\mathcal{L}X_n) &:= Y_n \\ (I + h\mathcal{L}X_n)X_n(I - h\mathcal{L}X_n) &=: Y_{n+1}. \end{aligned} \quad (4)$$

In this scheme, Y_n denotes the approximate solution at time t_n . This scheme preserves the spectrum of Y_0 and nearly conserves the Hamiltonian (1), indeed it is a Lie–Poisson integrator (see [9]). We observe that whenever Y belongs to a quadratic matrix Lie algebra

$$\mathfrak{g}_J = \{Y \in \mathbb{M}(N, \mathbb{C}) \mid YJ + JY^* = 0\}$$

for some fixed $J \in \mathbb{M}(N, \mathbb{C})$, and $\mathcal{L} : \mathfrak{g}_J \rightarrow \mathfrak{g}_J$ linear, equation (1) admits solutions in \mathfrak{g}_J . Indeed, the left-hand side of equation (1) is the differential of the inverse of the Cayley transform, which is known to preserve quadratic Lie algebras [3]. Of particular interest for applications to PDEs is the case of $J = I$, for which $\mathfrak{g}_J = \mathfrak{u}(N)$, the Lie algebra of the skew-Hermitian matrices. In section 4, we consider the Lie algebra $\mathfrak{su}(N)$, which consists of skew-Hermitian matrices with zero trace.

Remark 1. *It is not hard to check that the following equalities hold:*

$$\begin{aligned} Y_{n+1} &= Y_n + h \left[\mathcal{L} \left(\frac{Y_{n+1} + Y_n}{2} \right), \frac{Y_{n+1} + Y_n}{2} \right] + O(h^2) \\ X_{n+1} &= X_n + \frac{h}{2} ([\mathcal{L}X_{n+1}, X_{n+1}] + [\mathcal{L}X_n, X_n]) + O(h^2). \end{aligned} \quad (5)$$

Hence, up to a term of order $O(h^2)$, the Y_n evolve via the midpoint scheme, whereas the X_n via the trapezoidal scheme. It is known that the midpoint and the trapezoidal method are conjugate symplectic [3]. Hence, we have that X_n evolves accordingly to a scheme $\phi_h^T : X_n \mapsto X_{n+1}$ which is conjugate isospectral to the scheme $\phi_h^M : Y_n \mapsto Y_{n+1}$ as defined in (1), i.e. there exists an invertible map χ_h such that:

$$\phi_h^T = \chi_h^{-1} \circ \phi_h^M \circ \chi_h.$$

The map is clearly given by the left-hand side of the first equation in (1), which we denote as $\chi_h = \phi_{h/2}^{EE}$. We observe that $\chi_h = I + O(h)$. Hence, if Y_n evolves on a compact set, then X_n evolves on a compact set for any $n \geq 0$. We illustrate this relationship in the figure 1 below.

The need for an efficient solver for (1) can be understood by the fact that conservative PDEs, like the vorticity equation of fluid dynamics [10, 11] or the drift-Alfvén model for a quasineutral plasma [5], admit a spatial discretization in $\mathfrak{su}(N)$, for $N = 1, 2, \dots$. The crucial aspect of these finite-dimensional models is that they retain the conservation laws of the original equations. In order to retain these features, the resulting semi-discretized equations can be integrated in time using the scheme (1). Clearly, to get good spatial accuracy, N has to be quite large (at least 10^3). Moreover, the need for an efficient solver for (1) can be necessary for spin systems with many interacting particles. In this case, the equations (1) are posed in the product Lie algebra $\mathfrak{su}(2)^N$, where N is the number of

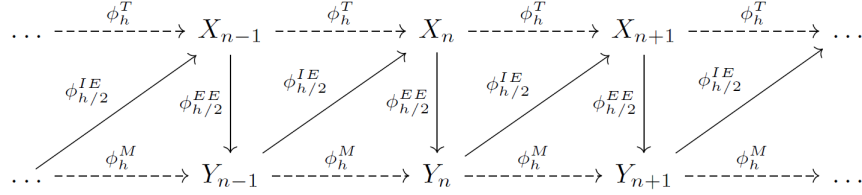


FIGURE 1. Illustration of the schemes (1), (1). Here ϕ_h^M denotes the map in the first line of (1), ϕ_h^T the map in the second line of (1), $\phi_{h/2}^{IE}$ the map in the first line of (1) and $\phi_{h/2}^{EE}$ the map in the second line of (1). Those correspond up to $O(h^2)$ terms respectively to the implicit midpoint, trapezoidal, implicit Euler, explicit Euler schemes.

particles. We stress that in a typical simulation, hundreds of these cubic matrix equations have to be solved to high accuracy. This paper is devoted to devise an efficient way to solve (1). First we prove existence and uniqueness of the solution for (1), for h sufficiently small. Then, we propose and investigate three possible algorithms to solve equation (1). First, in section 3.1 we consider a linear scheme, the convergence of which follows from the existence and uniqueness result. We will see in section 3.3 that a suitable inexact Newton method applied to (1) is also convergent, at least locally. We will see in section 3.2 that the third scheme, based on the Riccati equation is not practical, due to the non uniqueness of the solution. In the last section, we show the results of numerical experiments aimed at assessing the efficiency of the different schemes for various linear operators \mathcal{L} , which correspond to different physical models.

2. EXISTENCE AND UNIQUENESS

In this section, we show the existence and uniqueness of the solution for the equation (1), when the time-step h is sufficiently small.

Theorem 1. *Given $A \in M(N, \mathbb{C})$, equation (1) has a unique solution for some h in the interval $(0, \frac{1}{5\|Y\|\|\mathcal{L}\|_{op}})$, where $\|\mathcal{L}\|_{op}$ is the operator norm induced by the Frobenius norm, denoted with $\|\cdot\|$.*

Proof. We rewrite equation (1) as a fixed point problem $F(X) = X$, for

$$F(X) = (I - h\mathcal{L}X)^{-1}Y(I + h\mathcal{L}X)^{-1}.$$

We notice that F is defined and analytic for $h < 1/\|\mathcal{L}X\|$. In order to apply the Banach fixed point theorem, we have to derive the first order approximation for F . Let us compute the derivative for F :

$$\begin{aligned} F(X + Y) &= (I - h\mathcal{L}X - h\mathcal{L}Y)^{-1}Y(I + h\mathcal{L}X + h\mathcal{L}Y)^{-1} \\ &= (I - h(I - h\mathcal{L}X)^{-1}\mathcal{L}Y)^{-1}(I - h\mathcal{L}X)^{-1}Y \cdot \\ &\quad \cdot (I + h\mathcal{L}X)^{-1}(I + h\mathcal{L}Y(I + h\mathcal{L}X)^{-1})^{-1} \\ &= (I + h(I - h\mathcal{L}X)^{-1}\mathcal{L}Y)F(X)(I - h\mathcal{L}Y(I + h\mathcal{L}X)^{-1}) \\ &\quad + O(\|hY\|^2) \\ &= F(X) + h[(I - h\mathcal{L}X)^{-1}\mathcal{L}YF(X) - F(X)\mathcal{L}Y(I + h\mathcal{L}X)^{-1}] \\ &\quad + O(\|hY\|^2) \\ &= F(X) + hDF_X[Y] + O(\|hY\|^2), \end{aligned}$$

where $DF_X[\cdot] = (I - h\mathcal{L}X)^{-1}\mathcal{L}(\cdot)F(X) - F(X)\mathcal{L}(\cdot)(I + h\mathcal{L}X)^{-1}$. Hence, for $\|X - Y\|$ sufficiently small $F(X) - F(Y) = hDF_X[X - Y] + O(h^2\|X - Y\|^2)$. Hence, by the continuity of DF , there exists a neighbourhood U of X and an h sufficiently small such that F is a contraction on U .

The norm of DF_X can be estimated by:

$$\begin{aligned} \|DF_X\|_{op} &\leq 2\|\mathcal{L}\|_{op}\|(I - h\mathcal{L}X)^{-1}\| \|F(X)\| \\ &\leq 2\|\mathcal{L}\|_{op} \frac{1}{1 - h\|\mathcal{L}\|_{op}\|X\|} \frac{\|Y\|}{(1 - h\|\mathcal{L}\|_{op}\|X\|)^2} \\ &= \frac{2\|\mathcal{L}\|_{op}\|Y\|}{(1 - h\|\mathcal{L}\|_{op}\|X\|)^3}. \end{aligned}$$

In order for F to be a contraction we must have $h\|DF_X\|_{op} < 1$. Hence, it must be:

$$\begin{aligned} 2h\|\mathcal{L}\|_{op}\|Y\| &< (1 - h\|\mathcal{L}\|_{op}\|X\|)^3 \\ &= 1 - 3h\|\mathcal{L}\|_{op}\|X\| + 3h^2\|\mathcal{L}\|_{op}^2\|X\|^2 - h^3\|\mathcal{L}\|_{op}^3\|X\|^3. \end{aligned}$$

Since $\|X\| = \|Y\| + O(h)$, we get:

$$5h\|\mathcal{L}\|_{op}\|Y\| < 1 + O(h^2).$$

This completes the proof. \square

3. NUMERICAL SCHEMES

In this section, we present three possible numerical schemes to solve (1).

3.1. Linear scheme. Equation (1) can be decomposed into two coupled matrix equations. This splitting induces the following scheme:

$$\begin{aligned} P_k &:= \mathcal{L}X_k \\ (I - hP_k)X_{k+1} &:= Y, \end{aligned} \tag{6}$$

for $k = 1, 2, \dots$. Note that the second matrix equation in (3.1) is linear in the unknown matrix X_{k+1} . It is straightforward to check that $X_{k+1} = F(X_k)$, which we know from the previous section to be a contraction for h sufficiently small. Hence, the fixed point iteration has a unique solution for h small.

When $P \in \mathfrak{su}(N)$, we have $(I - hP)^* = (I + hP)$. Hence, it is enough to calculate the LU -factorization for $(I - hP)$ to have the one for $(I + hP)$. The resulting Algorithm 1 is given below. We observe that the cost per iteration is $O(N^3)$.

Algorithm 1 Explicit linear scheme in $\mathfrak{su}(N)$

Require: $Y \in \mathfrak{su}(N)$

$tol \leftarrow 10^{-10}$

$err \leftarrow 1$

$X_0 \leftarrow Y$

while $err > tol$ **do**

$P \leftarrow \mathcal{L}X_0$

$[L, U] = lu_factorization(I - hP)$

$X_1 \leftarrow U \setminus L \setminus Y/L^T/U^T$

$err \leftarrow \|X_1 - X_0\|$

$X_0 \leftarrow X_1$

end while

3.2. Quadratic scheme. Similarly, we can consider the same decomposition of the previous section for the equation (1), but reversing the roles of the known and unknown variables. This splitting induces the following scheme:

$$\begin{aligned} (I - hP_k)X_k(I + hP_k) &:= Y \\ \mathcal{L}X_{k+1} &:= P_k, \end{aligned} \quad (7)$$

where the unknown in the first equation is P_k . The first quadratic equation can be put in the form

$$h^2 PXP + h[P, X] + Y - X = 0, \quad (8)$$

which is a type of continuous algebraic Riccati equation (CARE).

Consider the case when equation (3.2) is posed in $\mathfrak{su}(N)$. Then we have two main issues concerning its solvability. On the one hand, defining $Z := (I - hP)$, we see that the first equation can be written as:

$$ZZ^* = Y. \quad (9)$$

Therefore, in order (3.2) to have solution, X and Y must be congruent. Hence, X_0 must be defined via some congruence transformation of Y . On the other hand, the following proposition shows that (3.2) admits infinitely many solutions. Let $I_{p,N-p}$ denote the diagonal matrix with the first p entries equal to 1 and the remaining $N - p$ entries equal to -1 , where $0 \leq p \leq N$. We denote by $U(p, N - p)$ the Lie group of matrices that leave the bilinear form $b(x, y) = x^* I_{p,N-p} y$ invariant.

Proposition 2. *Let $A, B \in \mathfrak{su}(N)$ be non-singular, with signature matrix equal to $I_{p,N-p}$. Then, the equation*

$$ZAZ^* = B \quad (10)$$

has solution $Z \in GL(N, \mathbb{C})$ if and only if $Z = CUD$, for some $U \in U(p, N - p)$ and C, D non-singular such that $B = CI_{p,N-p}C^$ and $DAD^* = I_{p,N-p}$.*

Proof. Let A, B, C, D be as in the hypotheses. Then, we can rewrite (2) as

$$C^{-1}ZD^{-1}I_{p,N-p}(C^{-1}ZD^{-1})^* = I_{p,N-p}.$$

Therefore, $C^{-1}ZD^{-1}$ is an element of $U(p, N - p)$. On the other hand, for any $U \in U(p, N - p)$, we have that $Z = CUD$ is a solution of (2). Hence, all the solutions of (2) have this form and are parametrized by $U \in U(p, N - p)$. \square

In our particular situation, we are interested in solutions of the form $Z = I + P$, for P skew-Hermitian. For instance, taking A, B diagonal such that $A - B \geq 0$, any P diagonal skew-hermitian (i.e. purely imaginary) such that $P^2 = BA^{-1} - I$ is a solution. Hence, for generic A, B as above, we get 2^N solutions, making the iteration (3.2) not well-defined.

We can see that the Riccati equation (3.2) has a non-uniqueness issue also in the following way. The equation can be split into two orthogonal components, one parallel to X and one orthogonal to it with respect to the Frobenius inner product:

$$\begin{aligned} h^2 \Pi_X(PXP) + \Pi_X Y - X &= 0 \\ h^2 \Pi_X^\perp(PXP) + h[P, X] + \Pi_X^\perp Y &= 0, \end{aligned}$$

where Π_X is the orthogonal projection onto $\text{stab}_X := \{A \in \mathbb{M}(N, \mathbb{C}) \text{ s.t. } [A, X] = 0\}$. If we write $P_\parallel := \Pi_X P$ and $P_\perp := \Pi_X^\perp P$, we get:

$$\begin{aligned} h^2 P_\parallel X P_\parallel + h^2 \Pi_X(P_\perp X P_\perp) + \Pi_X Y - X &= 0 \\ h^2 \Pi_X^\perp(P_\perp X P_\perp) + h^2 P_\perp X P_\parallel + h^2 P_\parallel X P_\perp + h[P_\perp, X] + \Pi_X^\perp Y &= 0. \end{aligned}$$

If these equations have a solution $(P_{\parallel}, P_{\perp})$, then we also have a solution $(-P_{\parallel}, P'_{\perp})$, where $P'_{\perp} = P_{\perp} + O(h^2)$. In $\mathfrak{su}(2) \cong \mathbb{R}^3$ this is easily seen, since the above scheme reads [9]:

$$\begin{aligned} h^2 p_{\parallel}(x \cdot p_{\parallel}) + \Pi_x y - x &= 0 \\ h^2 p_{\perp}(x \cdot p_{\parallel}) + h p_{\perp} \times x + \Pi_x^{\perp} y &= 0. \end{aligned}$$

where \times denotes the vector product and the matrices in $\mathfrak{su}(2)$ have been represented as vectors in \mathbb{R}^3 , via the standard isomorphism. Hence, we have the solutions:

$$\begin{aligned} p_{\parallel} &= \pm \sqrt{\frac{\|x\| - \|\Pi_x y\|}{h^2 \|x\|}} \frac{x}{\|x\|} \\ R p_{\perp} &= -\Pi_x^{\perp} y, \end{aligned}$$

where $R \in \mathbb{M}(3, \mathbb{R})$ is such that $R p_{\perp} = h^2 p_{\perp}(x \cdot p_{\parallel}) + h p_{\perp} \times x$. Hence, the ambiguity of the sign in p_{\parallel} causes a non-uniqueness of solution.

3.3. Cubic scheme. Newton's method can be directly applied to solve (1). A practical implementation is obtained rewriting (1) in the following way:

$$F(X) = X - h[\mathcal{L}X, X] - h^2(\mathcal{L}X)X(\mathcal{L}X) - Y = 0.$$

The Jacobian of F applied to a matrix Z is given by:

$$\begin{aligned} DF(X)[Z] = & Z - h([\mathcal{L}Z, X] + [\mathcal{L}X, Z]) \\ & - h^2((\mathcal{L}Z)X(\mathcal{L}X) + (\mathcal{L}X)Z(\mathcal{L}X) + (\mathcal{L}X)X(\mathcal{L}Z)). \end{aligned} \quad (11)$$

For h sufficiently small we have that $DF(X)^{-1} = (I - h\mathcal{B})^{-1} \approx (I + h\mathcal{B})$, for some operator \mathcal{B} acting on the space of matrices.. Then, we consider the following approximation for the inverse of the Jacobian:

$$\begin{aligned} DF(X)^{-1}[F(X)] &\approx \widetilde{DF}(X)[F(X)] \\ &:= F(X) + h([\mathcal{L}F(X), X] + [\mathcal{L}X, F(X)]) \\ &\quad + h^2((\mathcal{L}F(X))X(\mathcal{L}X) + (\mathcal{L}X)F(X)(\mathcal{L}X) + (\mathcal{L}X)X(\mathcal{L}F(X))). \end{aligned}$$

This approximation leads to the inexact Newton scheme (Algorithm 2) described below.

Algorithm 2 Inexact Newton scheme

Require: $A \in \mathfrak{su}(N)$

$tol \leftarrow 10^{-10}$

$err \leftarrow 1$

$X_0 \leftarrow Y$

while $err > tol$ **do**

$X_1 \leftarrow X_0 + \widetilde{DF}(X)[F(X_0)]$

$err \leftarrow \|X_1 - X_0\|$

$X_0 \leftarrow X_1$

end while

We observe that the Inexact Newton method above has its main computational cost in the evaluation of the approximated Jacobian (3.3), due to the several matrix-matrix multiplications required. Hence, for large N , the lower complexity of the scheme defined in Section 3.1 makes it more advantageous than the Inexact Newton's one, in terms of cost per iteration.

4. NUMERICAL EXPERIMENTS

In this section, we test our algorithms on three concrete examples arising from the numerical solution of spatially semi-discretized conservative PDEs: the incompressible Euler equations, the Drift-Alfvén plasma model, and the Heisenberg spin chain. To integrate in time the equations of motion, we apply the numerical scheme (1). For each equation, we test the performances of the schemes defined in sections 3.1 and 3.3. Here we briefly summarize our findings. For large time-step h , the scheme of section 3.1 is more efficient when solving (1) for large matrices. This makes the linear scheme more suitable for solving the Euler equations or the Drift-Alfvén plasma model. Analogously, we observe that for spin-systems, for large time-step and many particles, the scheme of section 3.1 is faster and has better convergence properties than the one of section 3.3.

We observe that for both the Euler equations and Drift-Alfvén plasma model, the number of iterations tends to decrease with increasing N . This is due to the fact that we are normalizing the initial values of the vorticity and the fact that we are absorbing into the time-step the factor $N^{3/2}$ which should multiply the matrix bracket in order to have spatial convergence of the right-hand side of equations (4.1) and (4.2) (see [6]). Indeed, the same phenomenon is not observed for the Heisenberg spin chain, where the spatial discretization is kept fixed while the number of particles is increased.

Another observation is that both in the Euler equations and in the Drift-Alfvén plasma model, the small number of Newton iterations for large N prevents any benefit from combining in series the two algorithms, i.e., using a few steps of the fixed point iteration to get a good initial guess for the inexact Newton scheme. Analogously, we have not observed any improvement in the convergence speed using a mixed scheme for the Heisenberg spin chain.

The simulations are run in Matlab2020a on a Dell laptop, processor Intel(R) Core(TM) i7-1065G7 CPU @ 1.30GHz 1.50 GHz, RAM 16.0 GB. For each simulation, a tolerance of 10^{-10} has been used as stopping criterion of the iteration. The results in the tables have been obtained as the average of 10 runs of the respective algorithm for solving equation (1), each run with respect to a different randomly generated Y . The CPU time is measured in seconds.

4.1. 2D Euler equations. The 2D Euler equations on a compact surface $S \subset \mathbb{R}^3$ can be expressed in the vorticity formulation as:

$$\begin{aligned}\dot{\omega} &= \{\psi, \omega\} \\ \Delta\psi &= \omega,\end{aligned}\tag{12}$$

where ω is the vorticity field, ψ is the stream function, the curly brackets denote the Poisson brackets, and Δ is the Laplace-Beltrami operator on S . Let us fix $S = \mathbb{S}^2$, the 2-sphere. Equations (4.1) admit a spatial discretization called *consistent truncation* (see [10, 11]), which takes the form:

$$\begin{aligned}\dot{W} &= [P, W] \\ \Delta_N P &= W,\end{aligned}\tag{13}$$

where $P, W \in \mathfrak{su}(N)$, for $N = 1, 2, \dots$ and for a suitable operator Δ_N . Since Δ_N can be chosen to be invertible, we get that equations (4.1) are of the form (1), with $\mathcal{L}W = \Delta_N^{-1}W$. Equations (4.1) are also a Lie–Poisson system, hence the scheme (1) is well-suited to retain its qualitative properties [3]. Clearly, in order to get a good approximation of the equations (4.1), we have to take N large (at least around 10^3 , see [6]).

In Table 4.1 we show the performances of the different schemes proposed in the previous section. We notice that for large N the linear scheme performs somewhat better than the inexact Newton one in terms of CPU time .

N	Fixed point iteration		Newton iteration	
	<i>Iterations</i>	<i>CPUtime</i>	<i>Iterations</i>	<i>CPUtime</i>
3	11.4	0.0018	6.3	0.0020
5	8.8	0.0021	5.4	0.0022
9	8.3	0.0017	4.7	0.0017
17	7.3	0.0024	4.4	0.0024
33	6.6	0.0041	3.7	0.0041
65	5.7	0.0071	3.3	0.0075
129	5.8	0.0163	3.1	0.0172
257	4.7	0.0517	3.3	0.0628
513	5.6	0.3268	3	0.3824
1025	5.9	1.8997	3	2.3771

TABLE 1. Solution of the Euler equation on the sphere. CPU time and number of iterations of the two proposed schemes, for time-step $h = 0.5$ and normalized randomly generated initial values.

4.2. Drift-Alfvén plasma model. The Drift-Alfvén plasma model [5] can be formulated in terms of the so called generalized vorticities ω_{\pm}, ω_0 . Although these are not directly physical quantities, they are a linear combinations of the generalized parallel momentum and the plasma density. In particular, neglecting the third order non-linearities, and absorbing the parameters in the time variable, we get the following equations:

$$\begin{aligned}
 \dot{\omega}_{\pm} &= \{\Phi_{\pm}, \omega_{\pm}\} \\
 \dot{\omega}_0 &= \{\Phi, \omega_0\} \\
 \Phi_{\pm} &= \Phi \pm \frac{1}{\lambda} \Psi \\
 \Delta \Phi &= \omega_+ + \omega_- + \omega_0 \\
 \Delta \Psi - \frac{1}{\lambda^2} \Psi &= \frac{1}{\lambda} \omega_+ - \frac{1}{\lambda} \omega_-,
 \end{aligned} \tag{14}$$

where λ is the ratio between the electron inertial skin depth and the ion sound gyroradius [5]. Analogously to the Euler equations, equations (4.2) have a matrix representation in $\mathfrak{su}(N) \times \mathfrak{su}(N) \times \mathfrak{su}(N)$, for any $N \geq 1$. If we assume $\omega_0 = 0$ (which physically means excluding the electrostatic drift vortices), we get:

$$\begin{aligned}
 \dot{\omega}_{\pm} &= \{\Phi_{\pm}, \omega_{\pm}\} \\
 \Phi_{\pm} &= \Phi \pm \frac{1}{\lambda} \Psi \\
 \Delta \Phi &= \omega_+ + \omega_- \\
 \Delta \Psi - \frac{1}{\lambda^2} \Psi &= \frac{1}{\lambda} \omega_+ - \frac{1}{\lambda} \omega_-.
 \end{aligned}$$

With the same notation of the previous section, we have the matrix equations:

$$\begin{aligned}
 \dot{W}_{\pm} &= [F_{\pm}, W_{\pm}] \\
 F_{\pm} &= F \pm \frac{1}{\lambda} P \\
 \Delta_N F &= W_+ + W_- \\
 \Delta_N P - \frac{1}{\lambda^2} P &= \frac{1}{\lambda} W_+ - \frac{1}{\lambda} W_-.
 \end{aligned} \tag{15}$$

Equations (4.2) can be cast in the form (1) in $\mathfrak{su}(N) \times \mathfrak{su}(N)$, for

$$\mathcal{L}(W_+, W_-) = (\Delta_N^{-1}(W_+ + W_-), \frac{1}{\lambda}(\Delta_N - \frac{1}{\lambda^2})^{-1}(W_+ - W_-)).$$

In Table 4.2, the performances of the two algorithms for the Drift-Alfvén model are reported. Analogously to the Euler equations, the linear scheme performs a bit better than the inexact Newton scheme, especially for large matrices.

N	Fixed point iteration		Newton iteration	
	<i>Iterations</i>	<i>CPUtime</i>	<i>Iterations</i>	<i>CPUtime</i>
3	10.8	0.0011	6	0.0016
5	9.6	0.0010	6	0.0013
9	8.1	0.0047	4.9	0.0029
17	7.5	0.0026	4.5	0.0032
33	6.7	0.0057	3.8	0.0063
65	5.9	0.0134	3.3	0.0145
129	5.4	0.0605	3.1	0.0622
257	6.3	0.3265	3.4	0.3607
513	4.4	1.3833	2.5	1.8628
1025	5.6	12.9432	3	17.1462

TABLE 2. Solution of the Drift-Alfvén model. CPU time and number of iterations of the two proposed schemes, for time-step $h = 0.5$, $\lambda = 5$, and normalized randomly generated initial values.

4.3. Heisenberg spin chain. The Heisenberg spin chain is a conservative model of spin particle dynamics. This model arises from the spatial discretization of the Landau–Lifshitz–Gilbert Hamiltonian PDE [4]:

$$\partial_t \sigma = \sigma \times \partial_{xx} \sigma, \quad (16)$$

where $\sigma : \mathbb{R} \times \mathbb{S}^1 \rightarrow \mathbb{S}^2$ is a closed smooth curve. Each value taken by σ in \mathbb{S}^2 represents a spin of an infinitesimal particle. We notice that unlike the previous examples of hyperbolic PDEs, equation (4.3) is a parabolic PDE. In Tables 4.3 and 4.3, we see that this requires a smaller time-step in order to have a comparable number of iterations of the two schemes as for the previous two examples.

Discretizing $\sigma \approx \{s_i\}_{i=1}^{N+1}$ on an evenly spaced grid with step size Δx of \mathbb{S}^1 , $\{x_i\}_{i=1}^{N+1}$, with the conditions $s_{N+1} = s_1$ and $x_{N+1} = x_1$, we obtain

$$\partial_{xx} \sigma(x_i) \approx \frac{s_{i-1} - 2s_i + s_{i+1}}{\Delta x^2}.$$

Each spin vector s_i can be represented by a matrix S_i with unitary norm in $\mathfrak{su}(2) \cong \mathbb{R}^3$. The equations of motion are given by:

$$\partial_t S_i = \left[S_i, \frac{S_{i-1} + S_{i+1}}{\Delta x^2} \right],$$

for $i = 1, \dots, N$. Hence, each spin interacts only with its neighbours (which explains the name chain). Hence, the matrices involved remain very sparse. A chain of N particles is an Hamiltonian system in $\mathfrak{su}(2)^N$, with Hamiltonian given by:

$$H(S_1, \dots, S_N) = \frac{1}{\Delta x^2} \sum_{i=1}^N \text{Tr}(S_i^* S_{i+1}).$$

In Tables 4.3 and 4.3, the results for the two algorithms are reported. In the numerical simulations, we set $\Delta x = 1$. We observe that the inexact Newton method does not converge for spin-systems with many particles and large time-step $h = 0.5$. On the other hand, the linear scheme does converge for any $N \leq 2^{10} + 1$, making it more suitable for long time simulations. For smaller time-step $h = 0.1$ the two algorithms perform almost equally well.

	Fixed point iteration		Newton iteration	
N	<i>Iterations</i>	<i>CPUtime</i>	<i>Iterations</i>	<i>CPUtime</i>
3	23	0.0008	39.4	0.0035
5	22.4	0.0013	129.3	0.0133
9	24.8	0.0011	308	0.0298
17	27.1	0.0017	NC	NC
33	27.4	0.0020	NC	NC
65	28.6	0.0040	NC	NC
129	30.4	0.0060	NC	NC
257	31.4	0.0130	NC	NC
513	32.2	0.0264	NC	NC
1025	33.1	0.0556	NC	NC

TABLE 3. Solution of Heisenberg spin chain model. CPU time and number of iterations of the two proposed schemes, for time-step $h = 0.5$ and normalized randomly generated initial values.

	Fixed point iteration		Newton iteration	
N	<i>Iterations</i>	<i>CPUtime</i>	<i>Iterations</i>	<i>CPUtime</i>
3	9	0.0003	6.5	0.0006
5	9.4	0.0004	7.3	0.0010
9	9.7	0.0005	7.4	0.0009
17	9.7	0.0007	8	0.0011
33	10.2	0.0013	8	0.0019
65	10	0.0015	8	0.0018
129	10.1	0.0021	8.5	0.0027
257	10.6	0.0041	8.3	0.0050
513	10.3	0.0097	8.7	0.0103
1025	10.9	0.0185	9	0.0192

TABLE 4. Solution of Heisenberg spin chain model. CPU time and number of iterations of the two proposed schemes, for time-step $h = 0.1$ and normalized randomly generated initial values.

5. CONCLUSIONS

In this paper we have proposed and investigated some iterative schemes for the solution of cubic matrix equations arising in the numerical solution of certain conservative PDEs by means of (Lie–Poisson) geometrical integrators. These types of schemes enable the preservation of important physical features of the original infinite-dimensional flows, which is generally not the case when more standard discretizations and numerical integrators are used. Both the fixed point and the inexact Newton type schemes we have investigated

tend to work well, but we found that the fixed point method is more robust with respect to the time step and tends to require less CPU time due to its lower computational cost per iteration.

REFERENCES

- [1] D. Bini, B. Iannazzo, and B. Meini. *Numerical Solution of Algebraic Riccati Equations*. SIAM, Philadelphia, 2012.
- [2] I. Gohberg, P. Lancaster, and L. Rodman. *Invariant Subspaces of Matrices with Applications*. SIAM, Philadelphia, 2006.
- [3] E. Hairer, C. Lubich, and G. Wanner. *Geometric Numerical Integration*. Springer, Berlin, Heidelberg, 2006.
- [4] M. Lakshmanan. The fascinating world of the Landau-Lifshitz-Gilbert equation: an overview. *Philosophical Transactions of the Royal Society A: Mathematical, Physical and Engineering Sciences*, 369:1280–1300, 2011.
- [5] J. H. Mentink, J. Bergmansa, L. P. J. Kamp, and T. J. Schep. Dynamics of plasma vortices: The role of the electron skin depth. *Physics of Plasmas*, 12, 052311, 2012.
- [6] K. Modin and M. Viviani. A Casimir preserving scheme for long-time simulation of spherical ideal hydrodynamics. *J. Fluid Mech.*, 884:A22, 2020.
- [7] Valeria Simoncini. Computational Methods for Linear Matrix Equations. *SIAM Review*, 58(3):377–441, 2016.
- [8] J. Sylvester. Sur l’equations en matrices $px = xq$. *C. R. Acad. Sci. Paris.*, 399 (2): 67–71, 1884.
- [9] M. Viviani. A minimal-variable symplectic method for isospectral flows. *BIT Num. Math.*, 60:741–758, 2020.
- [10] V. Zeitlin. Finite-mode analogues of 2D ideal hydrodynamics: Coadjoint orbits and local canonical structure. *Physica D*, 49(3):353–362, 1991.
- [11] V. Zeitlin. Self-Consistent-Mode Approximation for the Hydrodynamics of an Incompressible Fluid on Non rotating and Rotating Spheres. *Physical Review Letters*, 93(26):353–362, 2004.

Email address: `milo.viviani@sns.it`